

A SUBMILLIMETER BURST OF S255IR SMA1 - THE RISE AND FALL OF ITS LUMINOSITY

SHENG-YUAN LIU,¹ YU-NUNG SU,¹ IGOR ZINCHENKO,² KUO-SONG WANG,¹ AND YUAN WANG³

¹*Institute of Astronomy and Astrophysics, Academia Sinica, 11F of ASMA, AS/NTU No.1, Sec. 4, Roosevelt Road, Taipei 10617, Taiwan*

²*Institute of Applied Physics of the Russian Academy of Sciences, 46 Ul'yanov str., 603950, Nizhny Novgorod, Russia*

³*Max Planck Institute for Astronomy, Königstuhl 17, D-69117, Heidelberg, Germany*

(Received June 28, 2018; Revised July 21, 2018; Accepted July 26, 2018)

Submitted to ApJL

ABSTRACT

Temporal photometric variations at near infrared to submillimeter wavelengths have been found in low-mass young stellar objects. These phenomena are generally interpreted as accretion events of star-disk systems with varying accretion rates. There is growing evidence suggesting that similar luminosity flaring also occurs in high-mass star/cluster-forming regions. We report in this Letter the rise and fall of the 900 μm continuum emission and the newly found 349.1 GHz methanol maser emission in the massive star forming region S255IR SMA1 observed with the Submillimeter Array and the Atacama Large Millimeter/submillimeter Array. The level of flux variation at a factor of ~ 2 at the submillimeter band and the relatively short 2-year duration of this burst suggest that the event is probably similar to those milder and more frequent minor bursts seen in 3D numerical simulations.

Keywords: stars: protostars — stars: formation — ISM: individual objects (S255IR/S255IR SMA1)
— submillimeter: ISM

arXiv:1808.02192v1 [astro-ph.GA] 7 Aug 2018

1. INTRODUCTION

Temporal photometric variations associated with young low-mass stars of Class I or II, such as those FU Orion-type (FUor) and EX Lup-type (EXor) events, have been observed in the optical to mid-infrared (MIR) wavelengths (Audard et al. 2014). Accompanied by spectroscopic signatures of hot disks and winds, these phenomena are generally interpreted as accretion events of star-disk systems with elevated rates — instead of falling through steady flows to the central stars, circumstellar material fragments and accretes sporadically due to instabilities developed in the disks. Supplementary evidence includes the semi-periodic ejection events seen in the Herbig-Haro (HH) objects associated with low-mass young stellar objects (YSOs).

It is conceivable that at an earlier, more embedded (Class 0/I) evolutionary stage, YSOs may be subjected to similar episodic accretion events. Due to envelope obscuration, however, such phenomenon may not be visible in the optical or infrared (IR) but possibly detectable at longer (far-infrared (FIR) to millimeter) wavelengths (Johnstone et al. 2013). Indeed, HOPS 383, a Class 0 protostar, was the very first example reported with a brightening event not only in the MIR but also in the submillimeter bands (Safron et al. 2015). Furthermore, recent submillimeter observations of YSOs in nearby molecular clouds successfully revealed for the first time through a monitoring program a luminosity flaring event toward a Class I YSO in the Serpens cloud (Yoo et al. 2017). Molecular line imaging experiments, probing the thermal history of envelopes around embedded YSOs, also provided indirect indications of luminosity flarings (Jørgensen et al. 2013).

Does a similar luminosity variation phenomenon occur in the massive star formation process? There now appears to be growing evidence pointing to a positive answer. For example, the massive star-cluster-forming region S255 was first detected with methanol maser flares (Fujisawa et al. 2015). Subsequent observations in the near infrared (NIR) witnessed brightening of not only the NIR continuum but also atomic and molecular lines (Caratti o Garatti et al. 2017). NGC 6334(I), another massive star-cluster-forming site, also got spotted with an increase of its submillimeter continuum (Hunter et al. 2017). Follow-up observations confirm the emergence of new methanol masers as a result of the luminosity burst (Hunter et al. 2018).

S255IR is a massive cluster formation region with a bolometric luminosity of several $10^4 L_{\odot}$ at a distance of $1.78_{-0.11}^{+0.12}$ kpc (Burns et al. 2016). NIR imaging revealed a cluster of YSOs associated with the molecular gas ridge sandwiched by two nearby HII regions (Ojha et al.

2011). Submillimeter continuum observations indicated an overall molecular gas of around $300\text{--}400 M_{\odot}$ in this region, and disclosed at higher angular resolution several dense clumps residing in the complex (Wang et al. 2011; Zinchenko et al. 2012, 2015). In particular, the dominant source, S255IR SMA1, coinciding with the NIR source S255IR NIRS3, is associated with a prominent molecular bipolar outflow and a rotating disk-like structure (Zinchenko et al. 2012, 2015). The putative disk, perpendicular to the outflow in its orientation, probably is viewed closely edge-on (Boley et al. 2013). Based on its luminosity and the maser kinematics, the mass of the central YSO is estimated to be $\sim 20 M_{\odot}$ (Zinchenko et al. 2015). This region gained appreciable attention for its flaring signatures in 6.7 GHz methanol maser, NIR, and radio continuum (Fujisawa et al. 2015; Stecklum et al. 2016; Caratti o Garatti et al. 2017; Cesaroni et al. 2018) Meanwhile, Zinchenko et al. (2017) reported a newly identified submillimeter methanol maser, likely associated with this flare event, too.

2. OBSERVATIONS

This study utilizes observations with both the Submillimeter Array (SMA) and the Atacama Large Millimeter/submillimeter Array (ALMA). The SMA observations conducted in 2010 had been described in Zinchenko et al. (2015). The ALMA observations include three epochs, with the first two being introduced by Zinchenko et al. (2017). The third epoch of ALMA observations was carried out in the Cycle 4 Science Operation under #2015.1.00500.S. This last single execution block was conducted on 2017 July 20 when the 12 m array was in its C40-5 configuration with 43 antennas online. The projected baselines range between 15 m and 3.0 km. The same set of spectral windows in Zinchenko et al. (2017) are again employed. The continuum window is centered at 335.4 GHz with a bandwidth of 1875.0 MHz. The window at 349.0 GHz, covering the methanol maser, has a spectral channel width of 0.244 MHz and a resolution of 0.488 MHz (0.42 km s^{-1}) with online Hanning-smooth applied. J0854+2006 and J0750+1231 were used as the bandpass and flux calibrators, respectively, and J0613+1708 served as the complex gain calibrator. A compilation of key parameters for all observations are listed in Table 1.

The calibration and reduction of ALMA data were carried out with the Common Astronomy Software Applications (McMullin et al. 2007) and delivered by the observatory. Further imaging of the continuum emission is achieved by using the visibilities in the continuum window after obvious spectral contamination removed. Self-calibration were employed separately for different

observational epochs as described in Zinchenko et al. (2017) for improving the imaging quality and dynamical range. The antenna gain solutions were applied to both the continuum data as well as the 349.0 GHz spectral window.

3. RESULTS

3.1. Submillimeter dust continuum

3.1.1. SMA versus ALMA

Panels (a)–(b) in Figure 1 present the 900 μm continuum images of S255IR observed with SMA in 2010 December as reported in Zinchenko et al. (2015) and with ALMA in 2016 April. At a lower (SMA) resolution (panel (a)), two prominent features, S255IR SMA1 and SMA2, are resolved apart. S255IR SMA3 is further revealed in the higher resolution ALMA image (panel (b)). To compare the two observations fairly, we made mock SMA observations by re-sampling and imaging the ALMA map (panel (b)) using the uv -coverage achieved by the 2010 SMA observation, similar to the approach adopted in Hunter et al. (2017). In the resulting Figure 1(c), S255IR SMA1 and SMA2 remain visible in the mock image. The SMA image was taken at a slightly higher frequency (343 GHz) while the mock SMA image was taken at a lower frequency (335 GHz). Considering a typical spectral index of 3 for dust emission, one may expect the SMA image to be 7% brighter. However, it shows overall lower intensities. Instead of owing this to a negative spectral index, the discrepancy likely arises from the absolute flux calibration uncertainties, which can be as much as 20 – 30% for the SMA observations in particular. Furthermore, SMA1 and SMA2 show disparate contrasts in the two epochs, hinting on flux density variation in SMA1 and/or SMA2 during this period. It is very unlikely that the SMA1 flux remained constant, as this would imply absolute flux calibration errors being greater than 50%. Therefore, displayed in Figure 1(d) is the difference map between panels (a) and (c), if we assume that SMA2 has not changed. For that, (a) was scaled up by 20%, reasonably within calibration uncertainties, and subtracted from (c). A compact excess emission feature is visible in this difference map toward SMA1 while no obvious residual remains toward SMA2.

Given prior evidences of a flaring event associated with SMA1 in mid 2015, the above excess emission is most probably associated with this event. As listed in Table 1, the peak intensity in SMA1 rose from 0.50 Jy/beam in 2010 (after scaling) to 1.1 Jy/beam in 2016. The total flux density of SMA1, meanwhile, picked up from 0.73 Jy in 2010 (also after scaling) to 1.40 Jy in 2016. In brief,

both its intensity and flux density roughly doubled in 2016 as compared to 2010.

3.1.2. High-resolution imaging with ALMA

We present in Figure 2 the 900 μm continuum visibilities obtained with ALMA in 2016 April, 2016 September, and 2017 July. It is evident that between the first two epochs the visibilities at overlapping uv ranges are fully compatible, implying no variation toward S255IR during this period. On the other hand, variation (decreasing) of flux is evident in 2017 July. To localize this variation, we display in Figures 3 (a)–(b) the high ($0''.14$) resolution 900 μm continuum observed in 2016 September and 2017 July. For comparing these two observations, we generated synthesis images by using data within a common uv -range (14.5–1765 m) well shared by both observations and then restoring the final resolution to a circular $0''.14$ beam. Figure 3(c) is the difference map made by subtracting panel (b) from panel (a). While emission features such as SMA2 and SMA3 are canceled out, excess emission stands out noticeably at S255IR SMA1.

The peak intensity in S255IR SMA1, as observed in these maps, dropped from 0.237 Jy/beam, corresponding to a brightness temperature of 131 K, in 2016 September to 0.137 Jy/beam, or equivalently 76 K, in 2017 July. The flux density within a $0''.5$ aperture centered at SMA1 decreased by 33% during this interval.

3.2. Methanol maser emission

Zinchenko et al. (2017) reported a nonthermal methanol emission line at 349.1 GHz, reaching a brightness temperature of 3900 K (5.9 Jy/beam) at an angular resolution of $\sim 0''.12$. The line feature was assigned as a newly discovered maser associated with the $\text{CH}_3\text{OH } 14_1 - 14_0 A^{-+}$ transition, likely a Class II CH_3OH maser predominantly excited by IR radiation field. As indicated in Zinchenko et al. (2017), there was no indication of intensity variation in maser emission between 2016 April and September.

In Figure 4, the spectra at its peak position and the integrated intensity of the CH_3OH maser observed in 2016 September and 2017 July are presented. The peak intensities, though remaining nonthermal-like, has discernibly fallen to 2380 K (3.6 Jy/beam) in 2017 July, a reduction of 40%. The integrated intensity maps suggested no obvious shifts in the peak location within this period, while the difference map of the integrated intensity (Figure 4(c)) indicates that the excess CH_3OH emission region falls within the extent of the (excess) continuum emission delineated by the contour.

4. DISCUSSION

4.1. *A submillimeter flare, a manifestation of a luminosity burst*

As illustrated in the Section 3, the comparison between our SMA and ALMA observations indicated a factor of 2 increase in both the intensity and flux density of 900 μm continuum toward SMA1 in early 2016. ALMA observations further witnessed, for the first time, the waning of this continuum emission as well as CH_3OH maser in mid 2017.

No matter whether the dust continuum emission is optically thick or thin, its brightness and flux density variation is reflecting a dust temperature change, unless there is a dramatic modification in dust column density and/or opacity throughout the region. While an increase in luminosity may lead to enhanced sublimation of dust grains in the close vicinity ($\gtrsim 10$ au) of the central star and alter the heating timescale, the bulk dust properties likely remain similar (Hunter et al. 2017). The dust temperature elevated by a factor of ~ 2 in early 2016, thus suggests an overall bolometric luminosity increase by a factor of about 16 in S255IR SMA1 as total emission of the dust envelope scales with temperature to the 4th power (Hunter et al. 2017). For the short cooling timescale (of a few hundred seconds) of dust estimated from its heat capacity (Johnstone et al. 2013) and cooling rate (Glover & Clark 2012), the 88% dimming submillimeter continuum in 2016–2017, correspondingly a decreasing of dust temperature by 40%, also plausibly reflects a reduced radiation field, as well as a factor of ~ 8 decrease in its luminosity. Indeed, we witnessed fading (methanol) maser intensity along the same line of sight, most likely due to this reduction in seed radiation.

By investigating the NIR to submillimeter spectral energy distribution (SED) taken at the pre-burst phase and at 2016 February, Caratti o Garatti et al. (2017) unveiled a boost dominantly in the FIR at around 30–100 μm . The bolometric luminosity of S255IR SMA1/NIRS3 grew from $3 \times 10^4 L_\odot$ to $1.6 \times 10^5 L_\odot$, a factor of ~ 5.5 increase. This boost factor appears to be smaller than what we derived. Given that their FIR data are taken at angular resolutions coarser than $6''$, the inclusion of SMA2 and the surrounding material within those SED measurements probably resulted in lowering the boost factor. Furthermore, our luminosity estimation has a strong (fourth power) dependence on the dust temperature; a 10% uncertainty in the flux density, hence temperature measurement could lead to 40% uncertainty in the derived luminosity, which may partly mitigate the differences in the boost factors.

4.2. *The sequence of events*

Based on the propagation of the light echo, Caratti o Garatti et al. (2017) hypothesized that the S255IR SMA1 burst event occurred in mid-June of 2015. This appears consistent with the first report of 6.7 GHz methanol maser flaring seen from early July of 2015 as reported by Fujisawa et al. (2015). Direct NIR imaging in 2016 April disclosed brightening of the region as compared to the pre-burst image taken in 2009 (Caratti o Garatti et al. 2017). The extended K_s -band emission is the reprocessed light from hot dust presumably heated by the central star and escaped from the outflow cavity. Our ALMA image taken in 2016 April, meanwhile, also exhibits boosted submillimeter intensity toward SMA1 as compared to that of 2010. This emission presumably originates from the dusty disk and/or envelope, which remains optically thick to NIR and processes the radiation to longer wavelengths. Based on their Karl G. Jansky Very Large Array (VLA) monitoring observations, Cesaroni et al. (2018) further reported exponential flux flaring in the radio continuum between 6 and 45 GHz associated with SMA1 from 2016 July to 2017 February. This rising radio emission was interpreted as the radio jet breakout. Our 2017 July observation of both dust continuum and methanol maser subsequently indicates the dimming of this burst and marks the burst duration at around two years.

4.3. *Origin of the luminosity burst*

The fact that the submillimeter continuum emission brightened up and dimmed down in conjunction with Class II methanol maser activities in S255IR SMA1 is suggestive of variation in the IR radiation field and supports the notion of a disk-mediated accretion-related event as suggested by Caratti o Garatti et al. (2017). Indeed, on the large (10,000 au) scale, several lines of evidence point to the existence of a rotating structure associated with S255IR SMA1. Wang et al. (2011) and Zinchenko et al. (2012) demonstrated a velocity gradient perpendicular to the bipolar outflow in several molecular tracers, including CH_3CN , HCOOCH_3 , C^{18}O , and CH_3OH . While the angular resolution was not sufficient for a firm conclusion, the kinematic signatures of CH_3OH emission, including position-velocity diagram and velocity dispersion map, were both indicative of spin-up toward the inner region, reminiscent of Keplerian rotation (Zinchenko et al. 2015). MIR imaging by Boley et al. (2013) resolved an elongated dusty structure on a 1000 au scale perpendicular also to the bipolar outflow, possibly representing the putative circumstellar disk around S255IR SMA1. Caratti o Garatti et al. (2017) further reasoned that the accretion burst is disk-mediated based on the observed emission lines, such as H_2 , $\text{Br}\gamma$, as well as CO band-heads, He I, and Na I, typically seen as signatures of enhanced accretion, wind,

and hot disks in low-mass YSOs. The compact 900 μm continuum excess region seen in Figure 3(c) is likely associated with this structure.

Variable accretion is not uncommon in 3D numerical radiation hydrodynamic simulations of (low-mass and primordial) star formation (e.g. Vorobyov & Basu 2015; Hosokawa et al. 2016). Asymmetric features like spirals form in the circumstellar disk, which leads to fluctuating accretion rates. Moreover, Meyer et al. (2017) suggested the universal sporadic and variable nature of gaseous material accreting from the circumstellar disks to massive YSOs as in their low-mass counterparts. In their investigations of the collapse of 100 M_{\odot} pre-stellar cores, clumps of molecular gas spiraling from a few hundred au in the disk down to a few tens au from the central massive YSO and episodically accretes onto the star. In one particular case, the accretion rates and accompanying luminosity have major jumps up by nearly two orders of magnitudes for 10 years scale, while small variations in accretion rate and luminosity take place frequently. Such a disk fragmentation scenario was invoked as a possible cause leading to the quadruple luminosity burst seen toward NGC 6334(I) (Hunter et al. 2017).

For the low-mass star case, bursts of FUors and EXors are categorized with different characteristics. While FUor bursts typically arise with increases in mass accretion by several thousand folds and persist for years to decades, EXor bursts have enhanced mass accretion by factors of tens to hundreds and last for just months to years (Hartmann et al. 2016). Considering the relative mild magnitude and the short duration of the flare of S255IR SMA1, its temporal behavior resembles the milder and more frequent burst events, in analog to those seen in the EXors for low-mass YSOs. That being said, in an absolute sense, the scale of energy released by massive YSO events like this one in S255IR SMA1 or the burst seen in NGC 6334(I) (Hunter et al. 2017) is dramati-

cally different from the low-mass YSO cases. The luminosity of S255IR SMA1 at its burst stage, reaching $10^5 L_{\odot}$, corresponds to a mass accretion rate of several times $10^{-3} M_{\odot}$ (Caratti o Garatti et al. 2017). This is far more significant when compared with even the FUor bursts.

Based on the multiple scale outflows observed toward S255IR SMA1, Burns et al. (2016) conjectured an episodic accretion history over the last few thousand-year timescale. The most recent methanol maser and IR flare combined with our ALMA observations revealing the brightening and dimming signatures in submillimeter continuum further pointed out to an ongoing accretion burst. Monitoring observations of S255IR SMA1 in its continuum emission shall further constrain the full duration and degree of this latest burst. Meanwhile, supplementary molecular line observation could gauge the gas temperature, which should be subsequently warmed and cooled along the event, although the expected larger thermal time constant may imply a longer time lag and/or perhaps a milder strength in the gas temperature variation (Johnstone et al. 2013). Finally, high-angular-resolution imaging is essential for resolving the disk structure and revealing the burst nature of S255IR SMA1.

S.Y.L. acknowledges the support by the Minister of Science and Technology of Taiwan (MOST 106-2119-M-001-013). I.Z.'s research was supported by the Russian Science Foundation (grant No. 17-12-01256). This Letter makes use of the following ALMA data: ADS/JAO.ALMA #2015.1.00500.S. ALMA is a partnership of ESO (representing its member states), NSF (USA) and NINS (Japan), together with NRC (Canada), MoST and ASIAA (Taiwan), and KASI (Republic of Korea), in cooperation with the Republic of Chile. The Joint ALMA Observatory is operated by ESO, AUI/NRAO and NAOJ.

REFERENCES

- Audard, M., Ábrahám, P., Dunham, M. M., et al. 2014, *Protostars and Planets VI*, 387
- Boley, P. A., Linz, H., van Boekel, R., et al. 2013, *A&A*, 558, A24
- Burns, R. A., Handa, T., Nagayama, T., Sunada, K., & Omodaka, T. 2016, *MNRAS*, 460, 283
- Caratti o Garatti, A., Stecklum, B., Garcia Lopez, R., et al. 2017, *Nature Physics*, 13, 276
- Cesaroni, R., Moscadelli, L., Neri, R., et al. 2018, *arXiv:1802.04228*
- Fischer, W. J., Megeath, S. T., Tobin, J. J., et al. 2012, *ApJ*, 756, 99
- Fujisawa, K., Yonekura, Y., Sugiyama, K., et al. 2015, *The Astronomer's Telegram*, 8286,
- Galván-Madrid, R., Rodríguez, L. F., Liu, H. B., et al. 2015, *ApJL*, 806, L32
- Glover, S. C. O., & Clark, P. C. 2012, *MNRAS*, 421, 116
- Hartmann, L., Herczeg, G., & Calvet, N. 2016, *ARA&A*, 54, 135
- Hosokawa, T., Hirano, S., Kuiper, R., et al. 2016, *ApJ*, 824, 119
- Hunter, T. R., Brogan, C. L., MacLeod, G., et al. 2017, *ApJL*, 837, L29
- Hunter, T. R., Brogan, C. L., MacLeod, G. C., et al. 2018, *ApJ*, 854, 170
- Johnstone, D., Hendricks, B., Herczeg, G. J., & Bruderer, S. 2013, *ApJ*, 765, 133
- Jørgensen, J. K., Visser, R., Sakai, N., et al. 2013, *ApJL*, 779, L22
- McMullin, J. P., Waters, B., Schiebel, D., Young, W., & Golap, K. 2007, *Astronomical Data Analysis Software and Systems XVI*, 376, 127
- Meyer, D. M.-A., Vorobyov, E. I., Kuiper, R., & Kley, W. 2017, *MNRAS*, 464, L90

Table 1. Observing Parameters and SMA1 Measurements

Array	SMA	ALMA		
		2010 Dec 15	2016 Apr 21	2016 Sep 09
Observation date	2010 Dec 15	2016 Apr 21	2016 Sep 09	2017 Jul 20
Configuration	Compact	C36-2/3	C36(5)/6 [=C40-6]	C40-5
On-source time (minutes)	135	43	86	43
Antenna number	8	42	39	43
Minimum projected baseline (m)	9.1	12.1	12.0	14.6
Maximum projected baseline (m)	77	562	2811	3041
Continuum (imaging) freq. (GHz)	343.0	335.4	335.4	335.4
Continuum bandwidth (GHz)	2	1.875	1.875	1.875
SMA1 900 μm continuum				
peak brightness (Jy beam^{-1})	0.50 ^a	1.1 ^a	0.24 ^b	0.14 ^b
flux density (Jy)	0.73 ^c	1.4 ^c	0.64 ^d	0.41 ^d
SMA1 CH ₃ OH 14 ₁ – 14 ₀ A ^{–+} maser				
peak brightness (Jy/beam)		5.9 ^e	5.9 ^e	3.6 ^e

^aFor a $2''.3 \times 1''.9$ beam with a position angle -73°

^bFor a $0''.14 \times 0''.14$ beam

^cFor a $4''.0$ aperture

^dFor a $0''.5$ aperture

^eFor a $0''.14 \times 0''.14$ beam

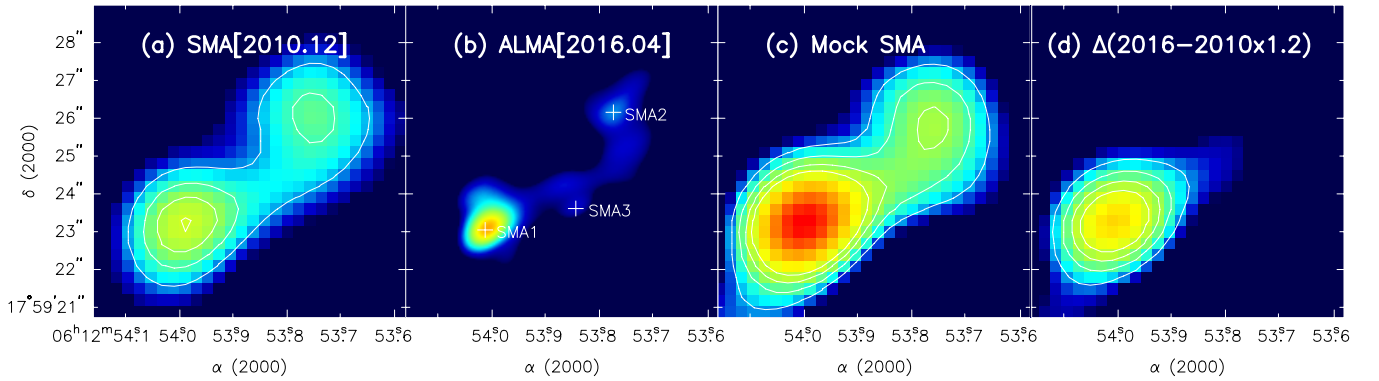


Figure 1. 900 μm continuum image of S255IR (a) observed in 2010 December by SMA at an angular resolution of $\sim 2''.0$. Contour levels are at $3, 5, 7,$ and 9×46 mJy/beam. (b) Observed in 2016 April by ALMA at an angular resolution of $\sim 0''.6$. The positions of SMA1–3 are marked by white crosses. (c) Made through mock SMA observations using panel (b) as the sky model. (d) The difference map made by first scaling panel (a) by 1.2 and subtracting that from panel (c). Contour levels in (c) and (d) are the same as (a), so does the false color scheme.

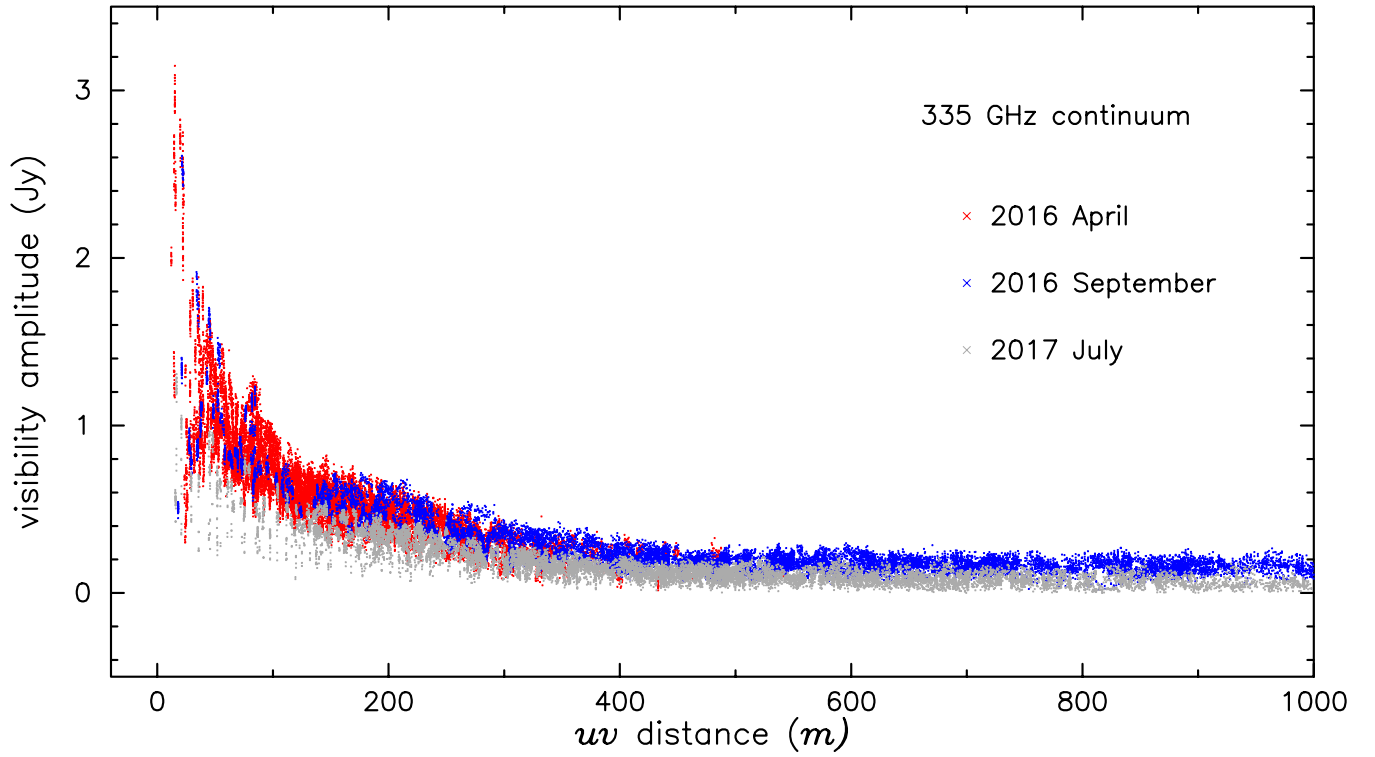


Figure 2. Visibility amplitudes of the 335 GHz continuum plotted against the uv -distance in meters. Red, blue, and gray points represent data taken with ALMA in 2016 April, 2016 September, and 2017 July, respectively.

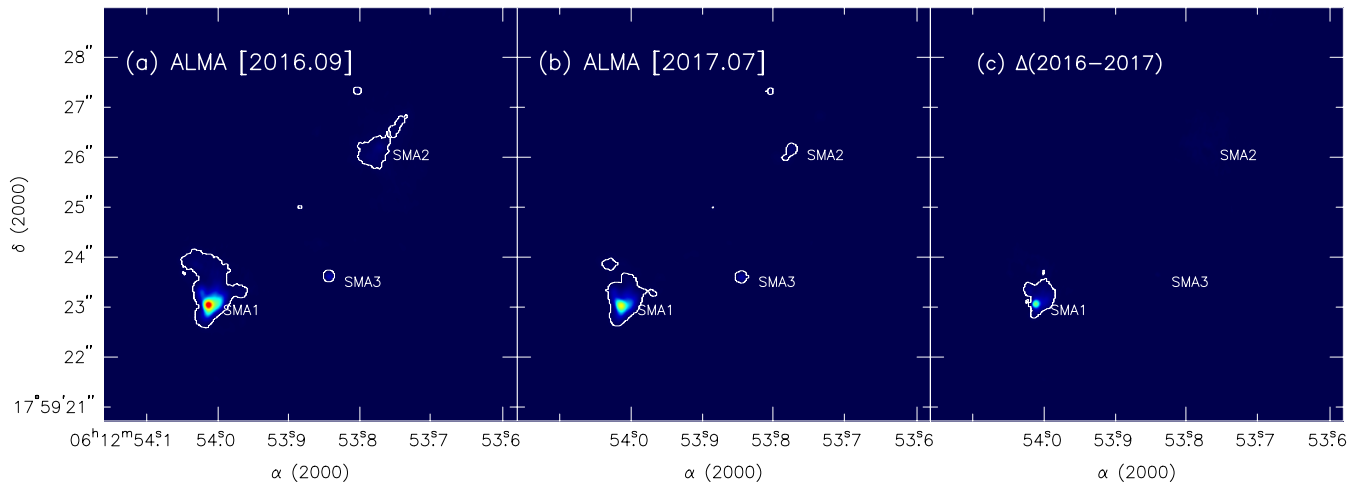


Figure 3. $900 \mu\text{m}$ continuum image of S255IR (a) observed in 2016 September by ALMA in false color at an angular resolution of $0''.14$. (b) Observed in 2017 July by ALMA at an angular resolution of $0''.14$. The contour and labels are the same as those in (a). (c) The difference map made by subtracting panel (b) from panel (a). The contour at $5\text{-}\sigma$ level marks the boundary of regions with significant emission and SMA1–3 are labeled in panel (a)–(c).

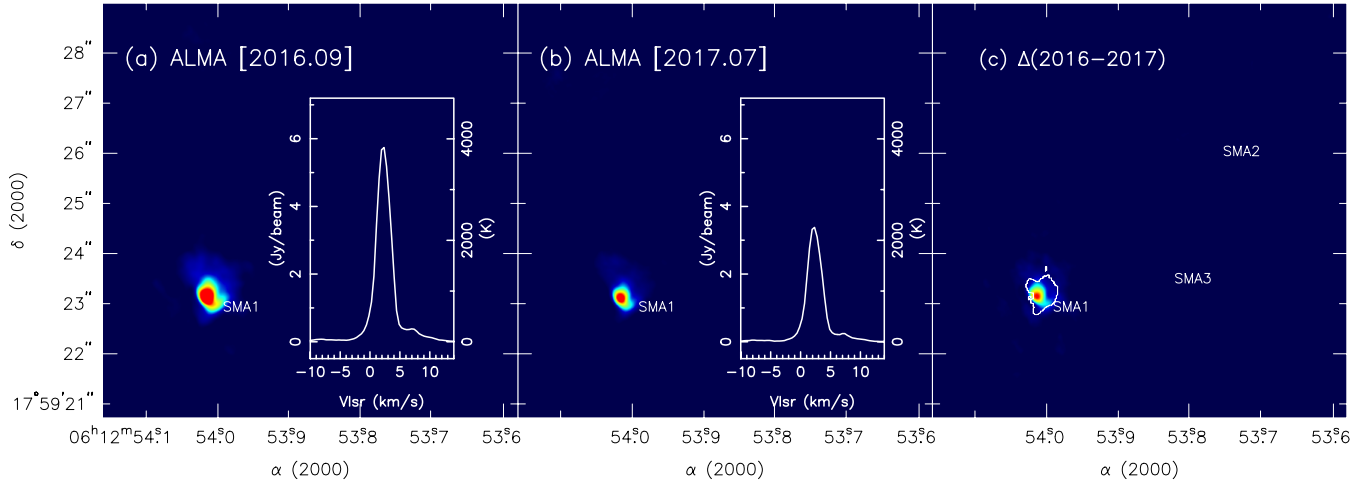


Figure 4. (a) Integrated intensity map of the 349.1 GHz $\text{CH}_3\text{OH } 14_1 - 14_0 A^{-+}$ maser emission observed by ALMA in 2016 September. An inset in the panel displays the CH_3OH spectra at its peak position. (b) The integrated intensity map of the same maser emission observed by ALMA in 2017 July. An inset, same as in panel (a), displays the peak position spectra. (c) The difference CH_3OH maser map made by subtracting panel (b) from (a). The contour delineates the region with excess 900 μm continuum emission shown in Figure 3(c).

Ojha, D. K., Samal, M. R., Pandey, A. K., et al. 2011, *ApJ*, 738, 156
 Safron, E. J., Fischer, W. J., Megeath, S. T., et al. 2015, *ApJL*, 800, L5
 Stecklum, B., Caratti o Garatti, A., Cardenas, M. C., et al. 2016, *The Astronomer's Telegram*, 8732,
 Vorobyov, E. I., & Basu, S. 2015, *ApJ*, 805, 115
 Wang, Y., Beuther, H., Bik, A., et al. 2011, *A&A*, 527, A32

Yoo, H., Lee, J.-E., Mairs, S., et al. 2017, *ApJ*, 849, 69
 Zinchenko, I., Liu, S.-Y., Su, Y.-N., et al. 2012, *ApJ*, 755, 177
 Zinchenko, I., Liu, S.-Y., Su, Y.-N., et al. 2015, *ApJ*, 810, 10
 Zinchenko, I., Liu, S.-Y., Su, Y.-N., & Sobolev, A. M. 2017, *A&A*, 606, L6